Mechanical properties and microstructure of *in situ* synthesized ZrB_2-ZrN_{1-x} composites

HAILEI ZHAO*, JIANLIN WANG
Department of Inorganic Nonmetallic Materials, University of Science and Technology Beijing, Beijing 100083, China
E-mail: hlzhao@mater.ustb.edu.cn

ZHIMING ZHU
Department of Mechanical Engineering, Tsinghua University, Beijing 100084, China

JIAN WANG
Department of Inorganic Nonmetallic Materials, University of Science and Technology Beijing, Beijing 100083, China

WEI PAN
Department of Material Science and Engineering, Tsinghua University, Beijing 100084, China

Published online: 17 February 2006

ZrB_2-ZrN_{1-x} composites were *in situ* synthesized from Zr and BN powders by hot-pressing at high temperatures. Thermodynamic calculation indicates that ZrN will be formed preferentially than ZrB_2 in Zr-BN system. Three samples with Zr/BN molar ratios of 3:2, 3.5:2 and 2:1 were investigated at temperatures above 1650°C. All mixtures of Zr and BN transformed to ZrB_2-ZrN_{1-x} composites completely without any other detectable phases. Nonstoichiometric zirconium nitride, ZrN_{1-x}, is supposed to be formed in 3.5:2- and 2:1-samples. The microstructural morphology of well-sintered ZrB_2-ZrN_{1-x} composites is characterized by quadrate column-shaped ZrB_2 distributed evenly in the interwoven acicular ZrN_{1-x} matrix. A certain amount of hollow rectangular-shaped ZrB_2 with open ends is found in 3.5:2-sample hot-pressed at 1700°C, while some large spherical particles with lots of acicular ZrN_{1-x} sticked on its surface are observed in 2:1-sample hot-pressed at 1800°C. Excessive Zr compared to the stoichiometric Zr/BN molar ratio of 3:2 will facilitate the densification process. Acicular ZrN_{1-x} is apparently beneficial to the improvement of bending strength and fracture toughness of ZrB_2-ZrN_{1-x} composites.

1. Introduction

Zirconium boride and nitride are promising materials for high temperature applications mainly for their high melting point, high hardness, low chemical reactivity, excellent electrical conductivity and superb thermal shock resistance. Also, the excellent wear resistance makes them the potential candidates for various coating materials [1]. The densification of pure ZrB_2 or ZrN powders, however, shows rather difficult due to the high melting point, strong covalent bond and high vapor pressure of the constituents [2]. Attempts to densify ZrB_2 without sintering aids or with the addition of boron resulted in rather low final densities [3]. Addition of metal and oxides may lead to the poor creep behavior and the presence of secondary phase that may affect the excellent electrical and thermal conductivities of ZrB_2- and ZrN-based composites. Relatively high densities are achieved only by pressure-assisted sintering procedures at temperatures higher than 1900°C [4, 5].

Fortunately, ZrB_2 and ZrN have many similar properties, which offer the possibility to prepare ZrB_2-ZrN composite instead of monolithic ZrB_2 or ZrN material. *In situ* synthesis process is a promising method for producing new materials with homogeneous, well-developed microstructures at relatively lower temperatures [6]. Considerable composites of metal borides and nitrides were

*Author to whom all correspondence should be addressed.
0022-2461
DOI: 10.1007/s10853-006-2870-x

fabricated via this approach, such as TiB_2-TiC [7], ZrB_2-ZrC [8], AlN-TiB_2 [9], SiC-TiB_2 [10], TiB_2-TiN [6] and $MoSi_2$-MoB_2 [11]. However, there is limited report concerning the synthesis of ZrB_2-ZrN composite [12]. In present work, ZrB_2-ZrN composites were prepared from BN and metallic Zr powders by *in situ* hot-pressing process. The aim of this work is to investigate the microstructure characteristics and the mechanical properties of ZrB_2-ZrN composites with different initial amounts of Zr.

2. Experimental

Commercially available BN (particle size <1 μm) and metallic Zr (particle size <50 μm) were used as starting materials. Three compositions with Zr/BN molar ratios of 3:2, 3.5:2 and 2:1 were selected to investigate the effect of Zr content on the densification, microstructure and mechanical properties of ZrB_2-ZrN_{1-x} composites. The corresponding mixtures of these three samples were hot-pressed at 1800, 1700 and 1650°C respectively, and the so-obtained composites are noted as ZBN1, ZBN2 and ZBN3. In order to make an insight into the temperature dependence of microstructure of ZrB_2-ZrN_{1-x} composite, the Zr/BN mixture with Zr/BN molar ratio of 2:1 was also sintered at 1800°C and referred to as ZBN4. The powder blends with different molar ratios of Zr:BN were mixed in ethanol with Al_2O_3 balls for 8 h in a plastic bottle and then dried with a rotary evaporator under reflux condition to prevent the batch segregation due to the significant difference in density between Zr and BN. The dried mixed powders were placed into a cold graphite die with BN coating and loaded to 15 MPa before increasing the temperature. The furnace was kept at a vacuum of about 10^{-4} torr below 900°C in order to remove absorbed gases from the powder surface, followed by the Ar gas inlet into the chamber. The different samples were hot-pressed at designated temperatures under 20 MPa for 2 h in a flowing Ar atmosphere.

The phase compositions of so-obtained composites were identified by X-ray diffraction (XRD) using Cu K_α radiation after removing the surface layers by grinding. Bulk density was measured by the Archimedes method. Density values of 6.09 g/cm^3 for ZrB_2 and 6.97 g/cm^3 for ZrN were used to calculate the theoretical densities of the obtained ZrB_2-ZrN_{1-x} composites. The specimens for mechanical testing were cut with an electrical discharge saw and ground with a diamond wheel, then the tensile surface of the specimens was polished with diamond slurries down to 1 μm and the edges were beveled. The bending strength was evaluated by three-point bending test with a specimen size of $3 \times 4 \times 36$ mm^3, and the bending load was applied parallel to the hot-pressing axis with span 30 mm and a crosshead speed of 0.5 mm/min. Fracture toughness (K_{IC}) at room temperature was determined by the indentation fracture method. The mechanical properties data were an average of three measurements. The fracture surfaces of composites were observed by scanning electron microscopy (SEM). The crystalline grains were determined by energy dispersive X-ray spectrometry (EDX).

3. Thermodynamic analysis

Under Ar atmosphere, the reaction between Zr and BN should be:

$$3Zr + 2BN = ZrB_2 + 2ZrN \quad (1)$$

The program of HSC Chemistry® for Windows [13] has been employed to perform the thermodynamic calculation. The Gibbs free energy ΔG_T^0 of reaction (1) at temperatures of 1650, 1700 and 1800°C are −488.794, −486.911 and −483.143 kJ, respectively. The large negative values of ΔG_T^0 indicate the thermodynamic possibility of the reaction. The phase stability diagrams of Zr-B-N system at 1600 and 1800°C are calculated and drawn in Fig. 1. We can see that ZrN will be formed at a relatively lower partial pressure of nitrogen compared to ZrB_2 that is formed at a relatively higher boron partial pressure. For the mixture of Zr and BN powders heated under Ar atmosphere after a vacuum treatment, the partial pressure of nitrogen and boron should be almost the same. Thus ZrN will be generated in the mixture preferentially than ZrB_2; this

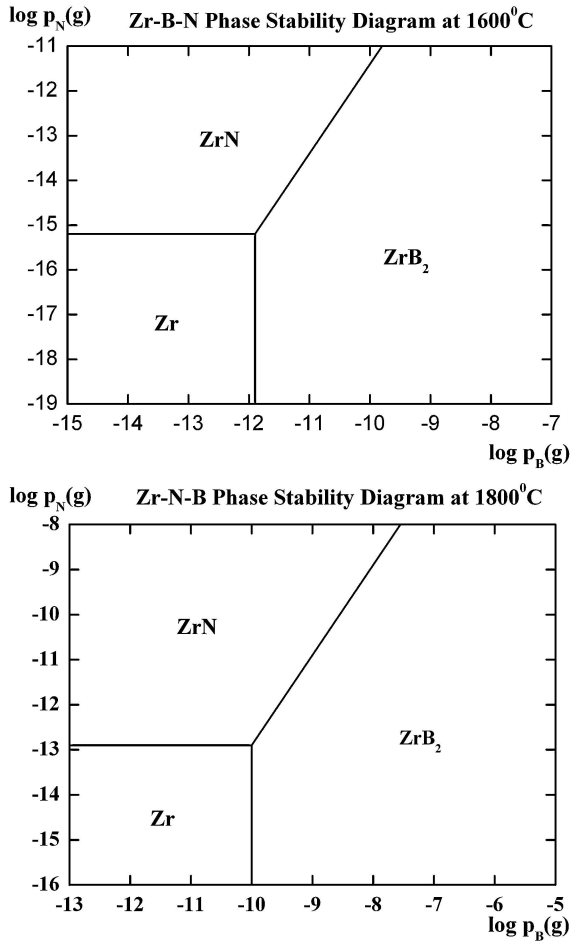

Figure 1 Phase stability diagrams of Zr-B-N system at 1600 and 1800°C.

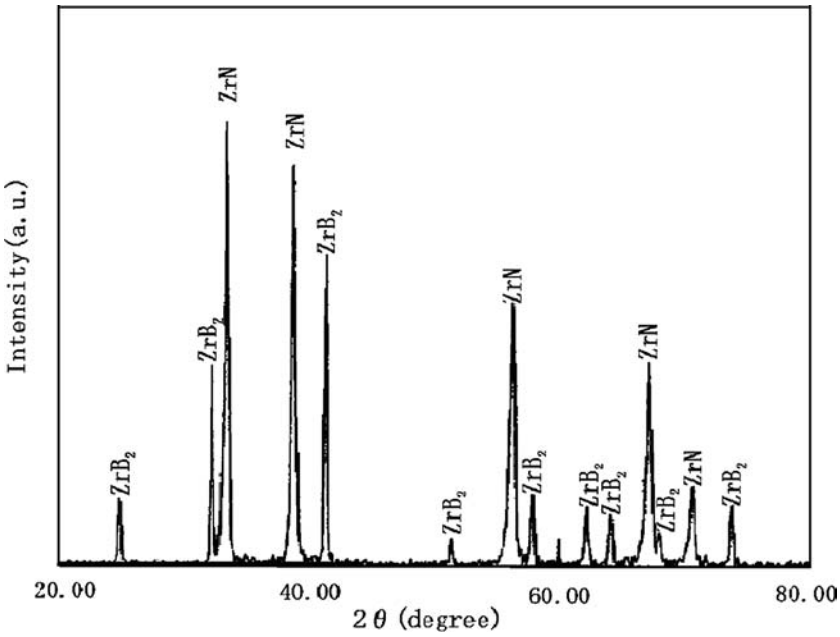

Figure 2 XRD pattern of sample ZBN2 after hot-pressed at 1700°C.

is consistent with our experimental result reported previously [14].

4. Results and discussion

XRD analysis shows that ZrB_2-ZrN composites have successfully synthesized. Only phases of ZrB_2 and ZrN were detected in all investigated samples, no any other phases were shown. Fig. 2 presents the XRD pattern of ZBN2. Because a quiet amount of excessive Zr exists in samples ZBN2 and ZBN3 compared to the stoichiometric ratio of Zr to BN in ZBN1 according to reaction (1), the pure ZrB_2-ZrN composites without any XRD peaks due to Zr implies that there is some nonstoichiometric compound in synthesized ZrB_2-ZrN composites. According to the literatures [15–17], nostoichiometric zirconium nitride with nitrogen vacancies is easily to be formed under low nitrogen partial pressure. Taking into account of the synthesis mechanism of the ZrB_2-ZrN composite described in our previous work [14], the reactions occurred in Zr/BN mixtures are likely to involve:

$$(3+y)\mathrm{Zr} + 2\mathrm{BN} \rightarrow \mathrm{ZrN}_{1-Z} + \mathrm{ZrB} + (2-m)\mathrm{BN}$$
$$+(3-n)\mathrm{Zr} \rightarrow (2+y)\mathrm{ZrN}_{2/(2+y)} + \mathrm{ZrB}_2 \qquad (2)$$

The resulting phases for hot-pressed ZBN1, ZBN2 and ZBN3 should be ZrB_2/ZrN, ZrB_2/$ZrN_{0.8}$ and ZrB_2/$ZrN_{2/3}$ respectively. Here we note the nonstoichiometric zirconium nitride as ZrN_{1-x}, where x is the nitrogen vacancies of the ZrN_{1-x} and is not accurately determined in present study.

SEM observation was conducted for all investigated samples. One of the most evident microstructural characteristics for samples ZBN1 and ZBN2 is that there are a large number of quadrate column-shaped grains distributed in interwoven acicular grains, as shown in Fig. 3. EDAX analysis indicates that the acicular grains correspond to ZrN_{1-x} and the quadrate column-shaped grains are due to ZrB_2. Interestingly, a certain amount of hollow tubular ZrB_2 is found in sample ZBN2, as presented in Fig. 4, which is much like the tubular mullite grains reported in Ref. [18]. The tubular ZrB_2 has square-framed or rectangular-framed cross-section with open end. They are not single-crystals but polycrystalline as a large amount of small particles appears in the exterior surface of tubular grains. The formation mechanism of tubular ZrB_2 is not clear so far, the nucleation and growth of the rectangular-framed tubular ZrB_2 certainly require systematic and extensive study.

Different from samples ZBN1 and ZBN2, sample ZBN3 shows matrix of small granular particles (~2 μm) with a lot of whisker-like ZrN_{1-x} on its surface (not shown here), although ZrN_{1-x} and ZrB_2 are the only detected XRD phases. The undeveloped microstructure of sample ZBN3 is considered to be due to the lower hot-pressed temperature compared to samples ZBN1 and ZBN2, where the elements can not get enough energy to realize the mass transfer and thus the grain growth to a perfect morphology.

In order to make an insight into the temperature effect on the microstructure, the Zr/BN blends with 2:1 molar ratio was hot-pressed at 1800°C for 2 h and the resultant product is noted as ZBN4. Contrary to sample ZBN3, a well-developed microstructure with rectangular column grains distributed in interwoven acicular grains exhibits in sample ZBN4. Besides, a little amount of large spherical particles is found in the matrix of sample ZBN4, which are actually aggregates of acicular ZrN_{1-x} grains, as evidenced in Fig. 5. The large spherical particle size is about

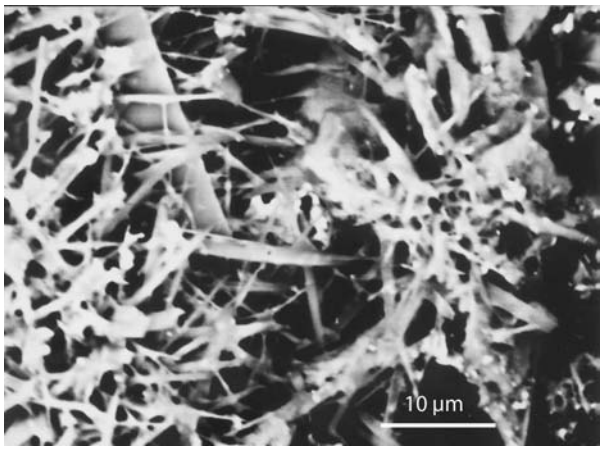

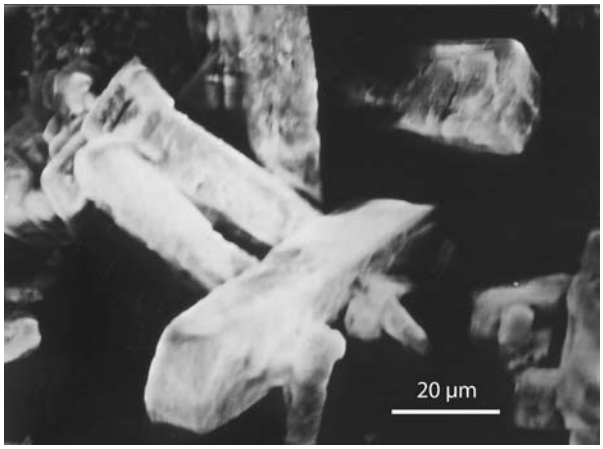

Figure 3 SEM micrographs of ZBN1 hot-pressed at 1800°C, showing acicular ZrN (a) and quadrate column-shaped ZrB_2 (b).

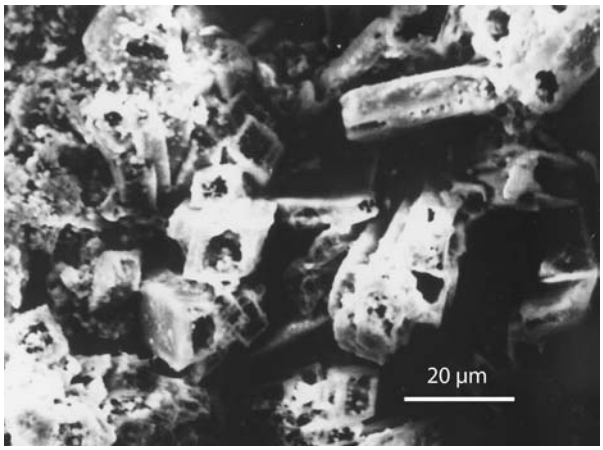

Figure 4 SEM photograph showing the hollow quadrate column-shaped ZrB_2 in sample ZBN2 hot pressed at 1700°C.

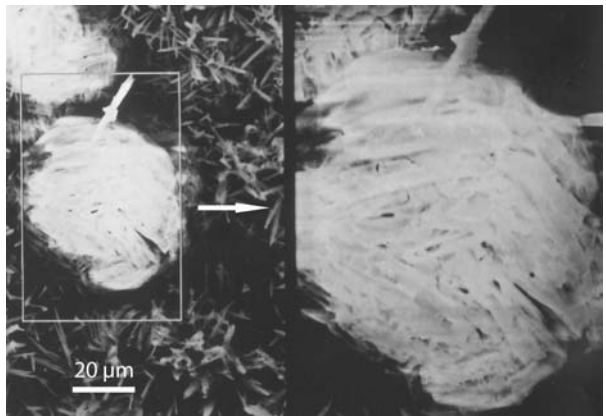

Figure 5 SEM photograph showing the large aggregates of acicular ZrN_{1-x} in sample ZBN4.

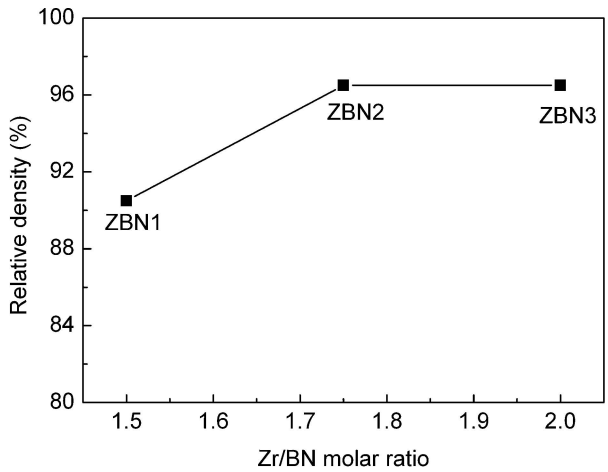

Figure 6 Variation of relative density of ZrB_2-ZrN_{1-x} composites in function of the Zr/BN ratio.

40 μm, equivalent to the particle size of starting metallic Zr. The formation of this spherical aggregate is deemed to be related with the melting of Zr particle. The thermodynamic calculation indicates that reaction (1) is an exothermic reaction with a large amount of enthalpy, −561.315 kJ at the temperature of 1800°C. A much higher local temperature is likely involved during the reaction sintering due to the reaction heat, which leads to a transient liquid phase of zirconium to enhance the densification [7]. The preferentially generated ZrN_{1-x} grains will stick on the surface of liquid Zr particle at the initial stage and then stretch towards the matrix with the continuous reaction between residual liquid Zr and boron. More liquid Zr will be formed in ZBN4 owing to its high Zr content. The large spherical particle with many acicular ZrN_{1-x} grains on its surface in sample ZBN4 is most likely to be due to the more excessive liquid Zr content. The interior part of the spherical large aggregates is supposed to be the unreacted metallic Zr, whose content should be below the detection limit of XRD.

Fig. 6 illustrates the relative density of hot-pressed samples ZBN1, ZBN2 and ZBN3 as a function of Zr/BN ratio. The relative density goes up with the increase of Zr/BN ratio although the hot-pressed temperature goes down with Zr/BN ratio, indicating that the excessive Zr compared to the stoichiometric Zr/BN ratio of 3:2 is more favorable to the densification process of *in situ* synthesized ZrB_2-ZrN_{1-x} composites. While, the effect tends to be not so obvious when Zr/BN ratio exceeds the value of 3.5:2. Nevertheless, sample ZBN1 achieves a relatively higher bending strength than samples ZBN2 and ZBN3,

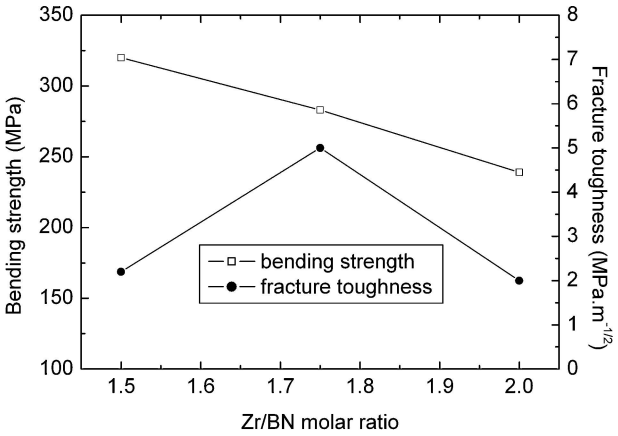

Figure 7 Variation of the bending strength and fracture toughness of samples ZBN1, ZBN2 and ZBN3 hot-pressed at 1800, 1700 and 1650°C, respectively.

as shown in Fig. 7. The bending strength of ZrB_2-ZrN_{1-x} composites varies adversely with the ratio of Zr to BN in starting compositions, whereas the fracture toughness increases remarkably as the Zr/BN ratio increases from 3:2 to 3.5:2. However ZBN3 exhibits quiet low fracture toughness. The degradation of bending strength with Zr content is very likely to be associated with the microstructure of ZrB_2-ZrN_{1-x} composite. The hollow tubular ZrB_2 in ZBN2 and the undeveloped particulate microstructure in ZBN3 should be responsible for the decrease in bending strength. The acicular ZrN is apparently favorable to the enhancement of fracture toughness of ZrB_2-ZrN_{1-x} composites. The high fracture toughness of sample ZBN2 is ascribed to the high ZrN_{1-x} content, while the low fracture toughness of sample ZBN3 is resulted from its particulate features. The acicular ZrN_{1-x} may easily allow the realization of crack bending during crack propagation and thus increase the energy consumption during fracture process.

ZNB4 shows a higher bending strength and fracture toughness compared to the other three samples, 458.8 MPa and 6.2 MPa $m^{-1/2}$ respectively for strength and toughness. The high relative density (98%) and the high acicular ZrN_{1-x} content (approximately of 75 mol%) of ZBN4 are believed to be responsible for this improvement.

5. Conclusions

ZrB_2-ZrN_{1-x} composites were *in situ* synthesized from Zr and BN powders with Zr/BN molar ratio of 3:2, 3.5:2 and 4:2 by hot-pressing at temperatures above 1650°C. All the mixtures of Zr and BN are transformed completely to ZrB_2 and ZrN_{1-x} phases without any other detectable phases, e.g. BN and Zr. Nonstoichiometric ZrN_{1-x} is supposed to exist in samples with Zr/BN molar ratio of more than 3:2. Nevertheless, excessive Zr apparently facilitates the densification process of ZrB_2-ZrN_{1-x} composites.

The typical microstructure characteristic of *in situ* synthesized ZrB_2-ZrN_{1-x} composites is that the quadrate column-shaped ZrB_2 distributes evenly in the interwoven acicular ZrN_{1-x} matrix. A certain amount of hollow rectangular ZrB_2 is found in 1700°C-sample with Zr/BN molar ratio of 2.5:2, while several large spherical particles with many acicular ZrN_{1-x} on its surface appear in 1800°C-sample with Zr/BN molar ratio of 2:1. The acicular ZrN_{1-x} is much favorable to the improvement of bending strength and toughness. A bending strength of 458.8 MPa and a fracture toughness of 6.2 MPa $m^{-1/2}$ are achieved by 1800°C-sintered sample with Zr/BN molar ratio of 2:1.

Acknowledgements

This work was kindly supported by State Key Laboratory of New Ceramics and Fine Processing, Tsinghua University, China.

References

1. E. KELESOGLE, C. MITTERER, M. K. KAZMANLI and M. ÜRGEN, *Surf. Coat. Technol.* **116-119** (1999) 133.
2. F. MONTEVERDE, A. BELLOSI and S. GUICCIARDI, *J. Euro. Ceram. Soc.* **22** (2002) 279.
3. D. N. ØVREBØ and F. L RILEY, in "Sixth-EcerS Conference & Exhibition, Extended Abstract, Vol.2. IOM Communications" (University Press, Cambridge, UK, 1999) p. 19.
4. C. MORZ, *Am. Ceram. Soc. Bull.* **74** (1995) 165.
5. R. HAYAMI, M. IWASA and M. KINOSHITA, *Yogyo-Kyokai-shi* **88** (1987) 352.
6. F. ØLEVSKY, P. MOGILEVSKY, E. Y. GUTMANAS and I. GOTMAN, *Metall. Mater. Trans. A* **27A** (1996) 2071.
7. G. WEN, S. B. LI, B. S. ZHANG and Z. X. GUO, *Acta Mater.* **49** (2001) 1463.
8. D. BRODKIN, S. R. KALIDINDI, M. W. BARSOUM and A. ZAVALIANGOS, *J. Am. Ceram. Soc* **79** (1996) 1945.
9. G. J. ZHANG and Z. Z. JIN, *Ceram. Int.* **22** (1996) 143.
10. G. J. ZHANG, Z. Z. JIN and X. M. YUE, *Mater. Lett.* **25** (1995) 97.
11. A. C. E. SILVA and M. J. KAUFMAN, *Intermetallics* **5** (1997) 1.
12. G. J. ZHANG, M. ANDO, J. F. YANG, T. OHJI and S. KANZAKI, *J. Euro. Ceram. Soc.* **24** (2004) 171.
13. A. ROINE, "Outokumpu HSC Chemistry for Windows, Ver. 5.11" (Outokumpu Research Oy, Pori, Findland, 2002).
14. H. ZHAO, J. WANG, W. QIU, J. WANG and W. PAN, in "Proceedings of Unitecr 2003 congress," (Osaka, Japan) p. 62
15. Y. GU, F. GUO, Y. QIAN, H. ZHENG and Z. YANG, *Mater. Lett.* **57** (2003) 1679.
16. H. M. BENIA, M. GUEMMAZ, G. SCHMERBER, A. MOSSER and J.-C. PARLEBAS, *Appl. Surf. Sci.* **200** (2002) 231.
17. T. YOSURYA, M. YOSHITAKE and T. KODAMA, *Cryogenics*, **37** (1997) 817.
18. X. Y. KONG, Z. L. WANG and J. WU, *Adv. Mater.* **15** (2003) 1445.

Received 18 February
and accepted 7 June 2005